Int. J. Heat Mass Transfer. Vol. 32, No. 1, pp. 157–169, 1989
Printed in Great Britain

0017-9310/89 $3.00+0.00

Comparison of turbulence models for the natural convection boundary layer along a heated vertical plate

R. A. W. M. HENKES and C. J. HOOGENDOORN
Department of Applied Physics, Delft University of Technology, P.O. Box 5046, 2600 GA Delft, The Netherlands

(*Received* 19 *February* 1988)

Abstract—With a numerical code for solving the boundary-layer equations, the performance of different turbulence models for the natural convection boundary layer for air along a heated vertical plate is tested. The algebraic Cebeci–Smith model, the standard k–ε model with wall functions for k and ε and different low-Reynolds number k–ε models are tested. The Cebeci–Smith model calculates a too low wall-heat transfer and turbulent viscosity. The standard k–ε model with wall functions gives a too high wall-heat transfer, but the velocity and temperature profiles agree reasonably with experiments. Accurate wall-heat transfer results require the use of low-Reynolds number k–ε models; the models of Lam and Bremhorst, Chien, and Jones and Launder perform best up to a Grashof number of 10^{11}. For larger Grashof numbers the Jones and Launder model is best. A sensitivity study shows that the wall-heat transfer with the standard k–ε model largely depends on the choice of the wall functions for k and ε. Replacing these wall functions by zero wall conditions for k and ε and adding the functions D and f_μ of the Chien model to the standard k–ε model gives a simple, but accurate low-Reynolds number k–ε model for the natural convection boundary layer.

1. INTRODUCTION

TIME AND length scales of a turbulent flow are often so small that in general the turbulence in the unsteady Navier–Stokes equations is further modelled. The two-equation k–ε model for turbulence is most widely used. This model is usually applied in combination with wall functions for the velocity and temperature close to a fixed wall to avoid the calculation of the steep gradients in the thin wall region. The wall functions also give boundary conditions for the differential equations for the turbulent kinetic energy k and the rate of dissipation of turbulent energy ε. In many flows the use of wall functions actually is not fully justified and Launder [1] has suggested that it might be 'time to abandon wall functions'. But in the thin wall region the turbulence is low, and the standard k–ε model has to be corrected for the low-Reynolds number effects. Different so-called low-Reynolds number k–ε models have been proposed in the literature.

Prandtl [2] showed that when the characteristic number of the flow, i.e. the Reynolds number for a forced convection flow and the Grashof (or Rayleigh) number for a natural convection flow, becomes infinitely large, some terms disappear from the Navier–Stokes equations, yielding the boundary-layer equations close to a fixed wall. To compare the performance of different low-Reynolds number k–ε models near to a wall, Patel *et al.* [3, 4] have solved the turbulent boundary-layer equations for a forced convection boundary layer, namely the flow along a flat plate in a uniform oncoming stream. A similar comparison will be made here for a natural convection boundary layer, namely the flow of air along a heated vertical plate placed in a stagnant, isothermal environment. Besides a comparison of the low-Reynolds number k–ε models, also comparisons will be given for the well-known algebraic model of Cebeci–Smith and the standard k–ε model with wall functions.

Using the standard k–ε model, a difficulty is that no good wall functions exist for the natural convection boundary layer. Recently George and Capp [5] and Cheesewright [6] have made some first proposals for these wall functions. At the moment natural convection computations still use the standard k–ε model with the logarithmic wall functions, which formally only hold for forced convection boundary layers with small pressure gradients. The sensitivity of the precise choice of these wall functions is investigated. Such a sensitivity study is also made for three low-Reynolds number k–ε models: the models of Lam and Bremhorst [7], Chien [8, 9] and Jones and Launder [10].

2. TURBULENT BOUNDARY-LAYER EQUATIONS

The time-averaged, two-dimensional, incompressible, turbulent boundary-layer equations are

$$\frac{\partial u}{\partial x}+\frac{\partial v}{\partial y}=0$$

$$\frac{\partial u^2}{\partial x}+\frac{\partial uv}{\partial y}=-\frac{1}{\rho}\frac{\mathrm{d}p}{\mathrm{d}x}+g\beta(T-T_\infty)+\frac{\partial}{\partial y}(\nu+\nu_t)\frac{\partial u}{\partial y}$$

$$\frac{\partial uT}{\partial x}+\frac{\partial vT}{\partial y}=\frac{\partial}{\partial y}\left(\frac{\nu}{Pr}+\frac{\nu_t}{\sigma_T}\right)\frac{\partial T}{\partial y}. \qquad (1)$$

NOMENCLATURE

$c_{1\varepsilon}, c_{2\varepsilon}, c_{3\varepsilon}$	coefficients in ε-equation
c_μ	coefficient in ν_t-equation
D	low-Reynolds number source term in k-equation
E	low-Reynolds number source term in ε-equation
f_1	low-Reynolds number correction for $c_{1\varepsilon}$
f_2	low-Reynolds number correction for $c_{2\varepsilon}$
f_μ	low-Reynolds number correction for c_μ
g	gravitational acceleration
G_k	buoyancy production of turbulent kinetic energy
Gr_x	local Grashof number, $g\beta\Delta Tx^3/\nu^2$
k	turbulent kinetic energy, $\overline{u_i'u_i'}/2$
Nu_x	local Nusselt number, $-x/\Delta T[\partial(T-T_\infty)/\partial y]_w$
p	pressure
P_k	shear production of turbulent kinetic energy
Pr	Prandtl number
Re_k	turbulent Reynolds number, $y\sqrt{k}/\nu$
Re_t	turbulent Reynolds number, $k^2/\nu\varepsilon$
T	temperature
ΔT	characteristic temperature difference, T_w-T_∞
T_τ	characteristic shear stress temperature, $-\nu(\partial T/\partial y)_w/Pr\,u_\tau$
T^+	dimensionless temperature, $(T_w-T)/T_\tau$
u	vertical velocity component
u_0	velocity scale, $(g\beta\Delta T\nu)^{1/3}$
u_τ	characteristic shear stress velocity, $\sqrt{(\nu(\partial u/\partial y)_w)}$
u^+	dimensionless velocity, u/u_τ
v	velocity component perpendicular to the plate
w	velocity component perpendicular to the u- and v-components
x	vertical coordinate beginning at the leading edge of the plate
x_b	beginning of the computational domain in the x-direction
x_{tr}	transition point
x_0	length scale, $(\nu^2/g\beta\Delta T)^{1/3}$
y	coordinate perpendicular to, and beginning at, the plate
y^+	dimensionless y-coordinate, yu_τ/ν.

Greek symbols

β	coefficient of thermal expansion
ε	rate of dissipation of turbulent kinetic energy, $\nu\overline{(\partial u_i'/\partial x_j)(\partial u_i'/\partial x_j)}$
ζ	dimensionless y-coordinate, yNu_x/x
ν	molecular kinematic viscosity
ν_t	turbulent kinematic viscosity
ρ	density
σ_k	turbulent Prandtl number for k
σ_T	turbulent Prandtl number for T
σ_ε	turbulent Prandtl number for ε.

Superscript

$'$	fluctuating quantity.

Subscripts

t	turbulent quantity
w	wall condition
∞	environment condition.

The Boussinesq approximation has been applied, implying that the density ρ is considered constant everywhere, except in the temperature buoyancy term, in which it is replaced by a linear dependence (constant coefficient of thermal expansion β) on the temperature difference $T-T_\infty$. An eddy viscosity model has been used to model the turbulent Reynolds stresses

$$-\overline{u'v'} = \nu_t\frac{\partial u}{\partial y}$$

$$-\overline{u'T'} = \frac{\nu_t}{\sigma_T}\frac{\partial T}{\partial y}. \tag{2}$$

The following models for the turbulent viscosity have been tested.

2.1. *Algebraic model of Cebeci–Smith*

Cebeci and Smith [11] used the following model to describe the turbulence in a forced convection boundary layer, which was modified by Cebeci and Khattab [12] for a natural convection boundary layer

$$\nu_t = \begin{cases} l^2|\partial u/\partial y|\gamma\gamma_{tr} \\ \quad \text{if } y < y_c \ (\nu_t \text{ is continuous at } y_c) \\ \alpha|\delta_2|\gamma\gamma_{tr} \\ \quad \text{if } y \geqslant y_c \text{ forced convection} \\ (0.075\delta_1)^2|\partial u/\partial y|\gamma\gamma_{tr} \\ \quad \text{if } y \geqslant y_c \text{ natural convection} \end{cases} \tag{3}$$

with

$$l = \kappa y[1-\exp(-y^+/A^+)] \text{ (Van Driest length)}$$

$$\kappa = 0.41 \text{ (Karman constant)}$$

$$y^+ = \frac{yu_\tau}{\nu}; \quad u_\tau = \sqrt{(\nu(\partial u/\partial y)_w)}$$

$$A^+ = 26/N; \quad N = \left(1-11.8\nu\frac{u_\infty}{u_\tau^3}\frac{du_\infty}{dx}\right)^{1/2}$$

$$\alpha = 0.0168\frac{1.55}{1+\pi};$$

$$\pi = 0.55[1-\exp(-0.243z_1^{1/2}-0.298z_1)]$$

$$z_1 = \frac{Re_\theta}{425} - 1,\ Re_\theta > 425;$$

$$Re_\theta = \frac{u_\infty}{v}\int_0^\infty \frac{u}{u_\infty}\left(1-\frac{u}{u_\infty}\right)\mathrm{d}y$$

$$\delta_2 = \int_0^\infty (u_\infty - u)\,\mathrm{d}y$$

δ_1 is the y-position of u_{95}; $|u_{95}-u_\infty| = 0.05u_{\max}$.

The factor γ is an intermittency factor, which accounts for the experimental observation that the boundary layer is turbulent at the outer edge during a fraction γ of time only

$$\gamma = 1\bigg/\left(1+5.5\left(\frac{y}{\delta_1}\right)^6\right).$$

This expression is used for forced convection boundary layers, whereas it is taken equal to 1 for natural convection boundary layers. γ_{tr} is a function to describe the transition from a laminar ($\gamma_{tr} = 0$) to a turbulent ($\gamma_{tr} = 1$) flow. From experiments it seems that a forced convection boundary layer becomes turbulent at a local Reynolds number of 1.5×10^6, and a natural convection boundary layer at a Grashof number of 2×10^9. The turbulent Prandtl number for temperature σ_T is taken as

$$\sigma_T = \frac{0.4(1-\exp(-y^+/A^+))}{0.44(1-\exp(-y^+/B^+))}$$

with

$$B^+ = \frac{1}{\sqrt{Pr}}\sum_{i=1}^{5} c_i(\log_{10}(Pr))^{i-1}$$

$$c_1 = 34.96,\quad c_2 = 28.79,\quad c_3 = 33.95,$$
$$c_4 = 6.33,\quad c_5 = -1.186.$$

2.2. *Standard k–ε model with wall functions*

Two differential equations are introduced to describe the kinetic energy of the turbulent velocity fluctuations k and the rate of turbulent energy dissipation ε

$$\frac{\partial uk}{\partial x} + \frac{\partial vk}{\partial y} = \frac{\partial}{\partial y}\left(v + \frac{v_t}{\sigma_k}\right)\frac{\partial k}{\partial y} + P_k + G_k - \varepsilon$$

$$\frac{\partial u\varepsilon}{\partial x} + \frac{\partial v\varepsilon}{\partial y} = \frac{\partial}{\partial y}\left(v + \frac{v_t}{\sigma_\varepsilon}\right)\frac{\partial \varepsilon}{\partial y}$$
$$+(c_{1\varepsilon}P_k - c_{2\varepsilon}\varepsilon + c_{1\varepsilon}c_{3\varepsilon}G_k)\frac{\varepsilon}{k} \quad (4)$$

with

$$P_k = v_t\left(\frac{\partial u}{\partial y}\right)^2,\quad G_k = -v_t g\beta\frac{\partial T}{\partial x},\quad v_t = c_\mu\frac{k^2}{\varepsilon}.$$

As a consequence of the boundary-layer simplifications used in this study, the buoyancy production term G_k can be neglected; Lin and Churchill [13] retained the term, after replacing the temperature's x-gradient by its y-gradient, to model fluids with a Prandtl number larger than 1 (water, oil).

Boundary conditions for k and ε at the wall are found from wall functions. It is known that close to a fixed wall velocity and temperature profiles in a forced convection boundary layer, with negligible pressure gradient, can be approximated by logarithmic wall functions

$$u^+ = \frac{1}{0.41}\ln(9y^+)$$

$$T^+ = 2.195\ln(y^+) + 13.2Pr - 5.66 \quad (5)$$

with

$$y^+ = \frac{yu_\tau}{v},\quad u^+ = \frac{u}{u_\tau},\quad T^+ = \frac{T_w - T}{T_\tau}$$

$$u_\tau = \sqrt{(v(\partial u/\partial y)_w)},\quad T_\tau = -\frac{v}{Pr\,u_\tau}\left(\frac{\partial T}{\partial y}\right)_w.$$

These wall functions can be used in the fully turbulent inertial sublayer at $y^+ > 11.5$. In the viscous sublayer close to the wall, $y^+ < 11.5$, turbulence can be neglected. Assuming that convection and molecular diffusion of k can be neglected in the inertial sublayer, the differential equation for k in equations (4) simplifies to

$$P_k = \varepsilon. \quad (6)$$

Hence, it is assumed that the production and dissipation of turbulent energy balances. Further, Prandtl's mixing length model is assumed to hold

$$v_t = (0.41y)^2\frac{\partial u}{\partial y}. \quad (7)$$

With the energy equilibrium (6), Prandtl's mixing length model (7) and the expression for v_t in the k–ε model (4), wall functions for k and ε are found

$$\frac{k}{u_\tau^2} = \frac{1}{\sqrt{c_\mu}}$$

$$\frac{v\varepsilon}{u_\tau^4} = \frac{1}{0.41y^+}\quad (y^+ > 11.5). \quad (8)$$

The wall function for k gives a boundary condition for the k-equation at the wall, whereas the wall function for ε gives a boundary condition for the ε-equation at the first inner computational grid point from the wall. The wall functions do not hold for forced convection boundary layers with large pressure gradients, natural convection boundary layers and if the condition $y^+ > 11.5$ is not satisfied. At the moment the development of a natural convection wall function for k and ε has not been completed yet; turbulent natural convection computational studies use wall functions like equations (8) to obtain boundary conditions for the standard k–ε model. Moreover, most natural convection calculations take the first inner computational grid point at $y^+ < 11.5$, where they do not use wall functions for the velocity and the temperature, but only use wall functions for k and ε.

2.3. *Low-Reynolds number k–ε models*

The standard k–ε model only holds if the local turbulence Reynolds number, i.e. a measure for the turbulence intensity ν_t/ν, is large. Close to the wall, e.g. this is not the case, and a modification of the model should be applied. Low-Reynolds number effects are modelled by the introduction of the functions f_1, f_2, f_μ, D and E

$$\frac{\partial uk}{\partial x}+\frac{\partial vk}{\partial y}=\frac{\partial}{\partial y}\left(\nu+\frac{\nu_t}{\sigma_k}\right)\frac{\partial k}{\partial y}+P_k-\varepsilon+D$$

$$\frac{\partial u\varepsilon}{\partial x}+\frac{\partial v\varepsilon}{\partial y}=\frac{\partial}{\partial y}\left(\nu+\frac{\nu_t}{\sigma_\varepsilon}\right)\frac{\partial \varepsilon}{\partial y}+(c_{1\varepsilon}f_1P_k-c_{2\varepsilon}f_2\varepsilon)\frac{\varepsilon}{k}+E \quad (9)$$

with

$$P_k=\nu_t\left(\frac{\partial u}{\partial y}\right)^2$$

$$\nu_t=c_\mu f_\mu\frac{k^2}{\varepsilon}.$$

Most low Reynolds number k–ε models, as summarized in Table 1, were originally developed for forced convection boundary layers. The last model in this table, the To and Humphrey [17] model, was developed for natural convection boundary layers. Lin and Churchill [13] used the Jones and Launder [10] model to calculate the natural convection boundary layer for air.

The results for the natural convection boundary layer do not strongly depend on the choice of the turbulent Prandtl number for the temperature σ_T. For example, increasing σ_T from 0.9 to 1.0 decreases the wall-heat transfer by 5%.

The choice of the functions f_1, f_2, f_μ, D and E should depend on the following considerations (see also Patel *et al.* [3, 4]).

2.3.1. *Experimental limit for small y.* For small y, the velocity fluctuations can be expanded according to

$$u'=a_1y+b_1y^2$$
$$v'=b_2y^2$$
$$w'=a_3y+b_3y^2. \quad (10)$$

With these series, k $(=\overline{u_i'u_i'}/2)$, ε $(=\nu\overline{\partial u_i'/\partial x_j\partial u_i'/\partial x_j})$ and ν_t $(=-\overline{u'v'}/(\partial u/\partial y))$ become (assuming homogeneous turbulence)

$$k=Ay^2+By^3+\ldots$$
$$\varepsilon=\nu(2A+4By+\ldots)$$
$$\nu_t=\frac{-\overline{a_1b_2}y^3+\ldots}{(\partial u/\partial y)_w} \quad (11)$$

with

$$A=(\overline{a_1^2}+\overline{a_3^2})/2,\quad B=\overline{a_1b_1}+\overline{a_3b_3}.$$

2.3.2. *D function and wall functions for k and ε.* Using series (11), the k-equation close to the wall reduces to

$$\nu\frac{\partial^2k}{\partial y^2}-\varepsilon+D=O(y^3) \quad (12)$$

with

$$\frac{\partial^2k}{\partial y^2}=2A+6By+\ldots.$$

All models apply $k=0$ as a wall condition, consistent with series expansion (11) for k. Not all models apply the non-zero value $\varepsilon=2\nu A$ as a wall condition; in order to satisfy equation (12) for at least the $O(1)$ terms, models applying $\varepsilon_w=0$ introduce a function D. Consequently, in that case the dissipation should be interpreted as $\varepsilon-D$, rather than as ε alone.

2.3.3. *f_2 and E functions.* Close to the wall the ε-equation reduces to

$$\nu\frac{\partial^2\varepsilon}{\partial y^2}-c_{2\varepsilon}f_2\frac{\varepsilon^2}{k}+E=O(y). \quad (13)$$

The choice for f_2 and E should be such that $\partial^2\varepsilon/\partial y^2=O(1)$ for small y. For example, if $E=0$ and a non-zero ε_w value is prescribed (implying that ε is $O(1)$ for small y), consistency is only found with $f_2=O(y^2)$ for small y. Some models introduce a non-zero E term, but its physical meaning is not very clear. Most models choose f_2 such that the decay of isotropic grid turbulence is modelled in agreement with experiments. These experiments show that the turbulent kinetic energy k decays as x^{-n}, with $n=1.25$ for large Re_t (i.e. for small x; $Re_t=k^2/\nu\varepsilon$) and $n=2.5$ for small Re_t (i.e. for large x). The decay is described by

$$\frac{\partial k}{\partial x}=-\varepsilon$$
$$\frac{\partial\varepsilon}{\partial x}=-c_{2\varepsilon}f_2\frac{\varepsilon^2}{k}. \quad (14)$$

Substitution of $k=c_1x^{-n}$ and $\varepsilon=c_2x^{-m}$ in equations (14) leads to

$$c_{2\varepsilon}f_2=\frac{n+1}{n}. \quad (15)$$

For $Re_t\to\infty$ all models have $f_2=1$, implying (with $n=1.25$) that $c_{2\varepsilon}$ should be 1.8. Indeed all models apply this value, or a value close to it. All models, except the Lam and Bremhorst [7] model, also approximately reproduce the low-Reynolds number decay limit, i.e. (with $n=2.5$) $f_2=1.4/c_{2\varepsilon}$ in the limit $Re_t\to 0$.

2.3.4. *f_μ function.* This function should be such that

Table 1. Constants and functions in the low-Reynolds number k–ε models

Model	ε_w	c_μ	$c_{1\varepsilon}$	$c_{2\varepsilon}$	σ_k	σ_ε	f_μ	f_1	f_2	D	E	σ_T
Standard k–ε with w.f.	w.f.	0.09	1.44	1.92	1.0	1.3	1.0	1.0	1.0	0	0	1.0
Lam and Bremhorst [7] (Dirichlet)	$\varepsilon = \nu \frac{\partial^2 k}{\partial y^2}$	0.09	1.44	1.92	1.0	1.3	$(1-\exp(-0.0165 Re_k))^2(1+20.5/Re_t)$	$1+\left(\frac{0.05}{f_\mu}\right)^3$	$1-\exp(-Re_t^2)$	0	0	0.9
Lam and Bremhorst (Neumann)	$\frac{\partial \varepsilon}{\partial y} = 0$	0.09	1.44	1.92	1.0	1.3	$(1-\exp(-0.0165 Re_k))^2(1+20.5/Re_t)$	$1+\left(\frac{0.05}{f_\mu}\right)^3$	$1-\exp(-Re_t^2)$	0	0	0.9
Chien [8, 9]	$\varepsilon = 0$	0.09	1.35	1.8	1.0	1.3	$1-\exp(-0.0115 y^+)$	1.0	$1-\frac{2}{9}\exp\left(-\left(\frac{Re_t}{6}\right)^2\right)$	$-2\nu\frac{k}{y^2}$	$-2\frac{\nu\varepsilon}{y^2}\exp(-0.5y^+)$	0.9
Hassid and Poreh [14]	$\varepsilon = 0$	0.09	1.45	2.0	1.0	1.3	$1-\exp(-0.0015 Re_t)$	1.0	$1-0.3\exp(-Re_t^2)$	$-2\nu\frac{k}{y^2}$	$-2\nu\left(\frac{\partial\sqrt{\varepsilon}}{\partial y}\right)^2$	0.9
Reynolds [15]	$\varepsilon = \nu \frac{\partial^2 k}{\partial y^2}$	0.084	1.0	1.83	1.69	1.3	$1-\exp(-0.0198 Re_k)$	1.0	$\left[1-0.3\exp\left(-\left(\frac{Re_t}{3}\right)^2\right)\right] f_\mu$	0	0	0.9
Hoffman [16]	$\varepsilon = 0$	0.09	1.81	2.0	2.0	3.0	$\exp\left(\frac{-1.75}{1+Re_t/50}\right)$	1.0	$1-0.3\exp(-Re_t^2)$	$-\frac{\nu}{y}\frac{\partial k}{\partial y}$	0	0.9
Jones and Launder [10]	$\varepsilon = 0$	0.09	1.44	1.92	1.0	1.3	$\exp\left(\frac{-2.5}{1+Re_t/50}\right)$	1.0	$1-0.3\exp(-Re_t^2)$	$-2\nu\left(\frac{\partial\sqrt{k}}{\partial y}\right)^2$	$2\nu\nu_t\left(\frac{\partial^2 u}{\partial y^2}\right)^2$	0.9
To and Humphrey [17]	$\varepsilon = 2\nu\left(\frac{\partial\sqrt{k}}{\partial y}\right)^2$	0.09	1.44	1.92	1.0	1.3	$\exp\left(\frac{-2.5}{1+Re_t/50}\right)$	1.0	$(1-0.3\exp(-Re_t^2)) f_3$	0	0	0.9

$$f_3 = \begin{cases} 1 & \text{if } y^+ \geqslant 5 \\ 1-\exp(-Re_t^2) & \text{if } y^+ < 5 \end{cases}$$

$Re_k = y\sqrt{k}/\nu$, $Re_t = k^2/\nu\varepsilon$, $y^+ = yu_\tau/\nu$.

HMT 32:1-K

the behaviour $\nu_t = O(y^3)$ in equations (10) is reproduced for small y. All models give a power of 3 or 4, with the exception of the Reynolds model which gives a power of 6 [15].

Some restrictions for the low-Reynolds number functions have been formulated. An inconsistency occurs for the Lam and Bremhorst model and for the Reynolds model; the consequences of these inconsistencies and the accuracy of all other models require a comparison with experiments.

3. NUMERICAL SOLUTION

The boundary-layer equations are solved for a semi-infinite heated vertical plate in a stagnant, isothermal environment. The variables are nondimensionalized with the length scale x_0, the velocity scale u_0 and the temperature scale ΔT $(= T_w - T_\infty)$. This leads to

$$\left\{\frac{u}{u_0}, \frac{v}{u_0}, \frac{T-T_\infty}{\Delta T}, \frac{k}{u_0^2}, \frac{x_0\varepsilon}{u_0^3}, \frac{\nu_t}{u_0 x_0}\right\} = f\left(\frac{x}{x_0}, \frac{y}{y_0}, Pr, \frac{x_0 g\beta\Delta T}{u_0^2}, \frac{\nu}{u_0 x_0}\right). \quad (16)$$

Because the geometry and boundary conditions in this natural convection problem do not define a length and velocity scale, they are formed with the coefficients $g\beta\Delta T$ and ν

$$x_0 = \left(\frac{\nu^2}{g\beta\Delta T}\right)^{1/3}$$

$$u_0 = (g\beta\Delta T\nu)^{1/3}. \quad (17)$$

With this choice the dimensionless solution only depends on Pr and on the following dimensionless coordinates:

$$\frac{x}{x_0} = \left(\frac{g\beta\Delta T x^3}{\nu^2}\right)^{1/3} = Gr_x^{1/3}$$

$$\frac{y}{y_0} = \left(\frac{g\beta\Delta T y^3}{\nu^2}\right)^{1/3} = Gr_y^{1/3}. \quad (18)$$

The following boundary conditions are applied:

$x = x_b$: laminar u- and T-profiles specified

$$x = x_{tr}: \frac{k}{u_0^2} = 0.647, \frac{\nu\varepsilon}{u_0^4} = \sqrt{c_\mu}\frac{k}{u_0^2}\left|\frac{\partial(u/u_0)}{\partial(y/x_0)}\right|$$

$$y = 0: u = v = 0, \frac{T-T_\infty}{\Delta T} = 1$$

k and ε specified by the considered k–ε model

$$y = y_\infty: u = 0, T = T_\infty$$

$$k \downarrow 0, \varepsilon \downarrow 0; \frac{\nu_t}{\nu} = c_\mu \frac{k^2}{\nu\varepsilon} = 20. \quad (19)$$

The calculations are started at $Gr_x = 10^9$, where the laminar similarity solution for the vertical plate is prescribed. Turbulence is introduced at $Gr_x = 2\times10^9$ by switching on the turbulence model, and introducing an amount of turbulent energy if a k–ε model is used. The outer edge of the computational domain is taken far enough to neglect its influence on the development of the boundary layer. Values of k and ε close to zero (but such that also k^2/ε remains small) are prescribed at this outer edge. The calculation is ended at $Gr_x = 10^{12}$.

The computational domain is covered with an equidistant grid in the x-direction and a non-equidistant grid in the y-direction. A v-grid point at an x-station is positioned just between two u-grid points (staggered grid). Grid points for the scalar variables coincide with the u-grid points. The x-derivatives are discretized with finite differences, whereas the y-derivatives are approximated with a finite-volume-like discretization. This discretization retains the characteristics of the finite volume/staggered grid discretization used for solving the Navier–Stokes equations as far as possible. Because the boundary-layer equations are parabolic they can be solved in a single sweep, going from one x-station to the next downstream station. An attempt was made to solve the system of non-linear equations at each x-station with the Newton–Raphson method. This method linearizes the equations at each iterative level, and solves the resulting block tri-diagonal matrix equation with a direct Gauss elimination. The method converges with a quadratic speed, which was checked for the laminar solution. The turbulence models are so complex that they were only partially linearized; still a fast convergence was found with the Cebeci–Smith model. The k–ε models, however, required a very accurate initial guess to prevent divergence. Our conclusion that the Newton–Raphson method is therefore unusable to solve the boundary-layer equations with a k–ε model agrees with Vanka's [18] experiences with this method to solve the Navier–Stokes equations with a k–ε model. Hence it was decided to use a segregated solution method; during an iteration the different differential equations in the boundary-layer equations are updated one after the other, solving only tri-diagonal matrix equations for each variable. Some underrelaxation was required to prevent divergence and obtain a reasonable speed of convergence.

Difficulties can arise to achieve a turbulent transition with a low-Reynolds number k–ε model. If the turbulence model is switched on at $Gr_x = 2\times10^9$, without introducing turbulent energy at this station or at the outer edge, the solution will remain laminar. If a ν_t-profile is prescribed at the first station upstream of $Gr_x = 2\times10^9$, the solution becomes turbulent. If such a profile is not prescribed, but instead a small non-zero ν_t is prescribed at the outer edge, a normal transition occurs at the 18×20 grid, a late transition is found at the 36×40 grid and there is no transition at the 72×80 grid. Once the solution has become turbulent, the solution at $Gr_x = 10^{12}$ is almost independent of the way the turbulence is introduced. The examples illustrate that the solution of the low-Reynolds number k–ε model is nonunique; assuming that the solution for large Gr_x is independent of the starting profile, both a laminar and turbulent solution exist for large Gr_x, applying homogeneous boundary conditions for k and ε at the wall and at the outer edge. This nonuniqueness can cause numerical problems. Ozoe *et al.* [19] tried to calculate the turbulent Navier–Stokes flow of water in a cavity heated from the side with the Jones and Launder model, setting k and ε to zero at all surfaces, but found that k and ε either converged to zero at all grid points or diverged.

All results to be presented in the sequel were made on a fine 72×80 grid, which was checked to give almost grid-independent results.

4. COMPARISON OF THE DIFFERENT MODELS

Patel *et al.* [3, 4] have compared the performance of some of the k–ε models (Table 1) for the forced convection boundary layer along a flat plate. In order to check our numerical code, these calculations have been repeated, and a perfect agreement has been found with their tabulated wall-shear stress coefficients. The natural convection boundary layer was calculated by Cebeci and Khattab [12], using the Cebeci–Smith model, by Lin and Churchill [13], using the Jones and Launder model, and by To and Humphrey [17] with their own model. Present results agree up to a graphical accuracy, except for the results with the To and Humphrey model, which considerably deviate.

Evaluation of the experiments for air at large Grashof numbers [6, 20–25] gives the following best fit curves for the wall-heat transfer coefficient and the velocity and temperature profiles

$$Nu_x = 0.106 Gr_x^{1/3}$$

$$\frac{u}{u_0} = \begin{cases} 54\zeta - 44\zeta^2(1 - 1/3\xi) & \text{conductive/thermo-viscous sublayer} \\ 39.7\zeta^{1/3} - 14.5 & \text{buoyant sublayer} \\ 4.34\ln\zeta - 3.13\zeta + 0.57\zeta\ln\zeta + 24.3 & \text{fully turbulent layer} \end{cases}$$

$$\frac{T - T_\infty}{\Delta T} = \begin{cases} 1 - \zeta & \text{conductive/thermo-viscous sublayer} \\ 0.63\zeta^{-1/3} - 0.23 & \text{buoyant sublayer} \\ 0.28 - 0.08\ln\zeta & \text{fully turbulent layer.} \end{cases} \quad (20)$$

The expression for the wall-heat transfer fits the experiments in the Grashof number range 5×10^{10}–10^{12}, and the velocity and temperature profiles fit the experimental range 5×10^{10}–5×10^{11}. The Nusselt number Nu_x and the length scale ζ are defined as

$$Nu_x = -x\left(\frac{\partial}{\partial y}\left(\frac{T - T_\infty}{\Delta T}\right)\right)_w$$
$$\zeta = \frac{yNu_x}{x}. \quad (21)$$

As shown by George and Capp [5] and Cheesewright [6], the coordinate ζ seems to be a similarity length scale of the turbulent natural convection boundary layer, giving a Gr_x-independent solution for u/u_0 and $(T - T_\infty)/\Delta T$ in the limit $Gr_x \to \infty$. Close to the outer edge the ζ-coordinate is not expected to be the right similarity scaling.

Our calculated wall-heat transfer for the different models is shown in Fig. 1 as a function of Gr_x. The results at $Gr_x = 10^{11}$ are summarized in Table 2. In particular the standard k–ε model with wall functions gives a too high result and the Cebeci–Smith model a too low result. Using the Lam and Bremhorst model, the results with the Dirichlet and Neumann boundary condition for ε at the wall are indistinguishable. The models of Lam and Bremhorst, Chien, and Jones and Launder are the low-Reynolds number k–ε models which are closest to the experiment up to $Gr_x = 10^{11}$. For larger Grashof numbers the wall-heat transfer according to the models of Lam and Bremhorst and Chien becomes a bit too high. However, the Jones and Launder model remains close to the experiment.

The velocity and temperature at $Gr_x = 10^{11}$ is compared with experiments in Fig. 2. The velocity maximum with the Cebeci–Smith model and with the standard k–ε model with wall functions is too high. None of the models is close to the experimental curves in the whole ζ range. Concerning the models of Lam and Bremhorst, Chien, and Jones and Launder it is noticed that they all fall above the experiments in the region close to the outer edge of the boundary layer. The Chien model is closest to the experimental temperature near the wall in the buoyant sublayer ($0.1 < \zeta < 1$). The velocity maximum in the Jones and Launder model is a bit too high.

The turbulent quantities k/u_0^2, $\nu\varepsilon/u_0^4$ and ν_t/ν are compared in Fig. 3. For all models (except for the standard k–ε model with wall functions, the To and Humphrey model and the Hoffman model) the qualitative picture is the same: the turbulent kinetic energy k forms a plateau around the position of the velocity maximum and reaches its maximum close to the outer edge, where the turbulent viscosity also reaches its maximum. The turbulent dissipation rate ε reaches its maximum just a bit nearer to the wall than the velocity. The low values of the turbulent viscosity ν_t found with the Cebeci–Smith model and the Hoffman model correspond with the laminar-like looking velocity profiles in Fig. 2(a), i.e. thin with a large velocity peak.

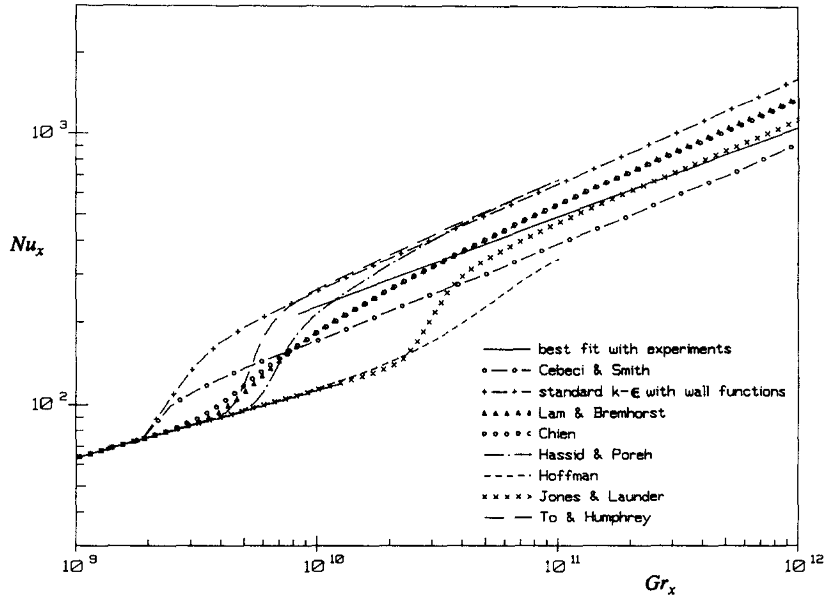

FIG. 1. Calculated wall-heat transfer ($Pr = 0.72$).

Table 2. Wall-heat transfer at $Gr_x = 10^{11}$ ($Pr = 0.72$)

Model	Nu_x
Experiment	492†
Cebeci–Smith	389
Standard k–ε with w.f.	642
Lam and Bremhorst (Dirichlet)	541
Lam and Bremhorst (Neumann)	541
Chien	543
Hassid and Poreh	679
Reynolds	‡
Hoffman	345
Jones and Launder	465
To and Humphrey	679

† According to the best fit curve $Nu_x = 0.106Gr_x^{1/3}$; e.g. 455 according to Siebers *et al.* [25], and 514 according to Miyamoto *et al.* [23].

‡ No converged solution could be obtained.

5. SENSITIVITY OF THE MODEL PARAMETERS

The influence of the choice of the boundary conditions for k and ε in the standard k–ε model has been checked. Hence, the following values for k and ε at the first inner grid point have been varied

$$k_w = \frac{u_\tau^2}{\sqrt{c_\mu}}, \quad \varepsilon_w = \frac{u_\tau^3}{0.41y}. \qquad (22)$$

The calculated wall-heat transfer on a 36×40 grid is shown in Fig. 4. It is seen that a minimum is reached close to the original choice, equations (22), giving a wall-heat transfer which is 29% above the experimental value. Decreasing ε_w and/or increasing k_w, i.e. increasing the turbulent viscosity at the first inner grid point, drastically increases the wall-heat transfer. Some natural convection studies [19, 26] use boundary conditions slightly different from equations (22)

$$k_w = 0 \qquad \text{at the wall}$$

$$\varepsilon_w = \frac{c_\mu^{3/4} k^{3/2}}{0.41y} \qquad \text{at the first inner gridpoint.} \qquad (23)$$

The influence of varying these values is depicted in Fig. 5. The original choice, equations (23), leads to a wall-heat transfer which is 51% above the experimental value. Decreasing ε_w largely increases the wall-heat transfer. Increasing ε_w decreases the wall-heat transfer until a 43% too large value is found for $\varepsilon_w \to \infty$.

A sensitivity study is also made for the low-Reynolds number k–ε models of Lam and Bremhorst, Chien, and Jones and Launder, which turned out to agree best with the experiments in the preceding section. The influence of the different terms in these models is given in Table 3. In all three models the trivial choice $f_2 = 1$ does not alter the wall-heat transfer. Further, the interchange of a non-zero boundary condition for ε with a non-zero D term nearly influences the wall-heat transfer. Setting $\varepsilon_w = 0$ (with $D = 0$) in the Lam and Bremhorst model or setting $D = 0$ (with $\varepsilon_w = 0$) in the Jones and Launder model also leads to only small changes; decreasing $|D|$ (with $\varepsilon_w = 0$) in the Chien model, however, enormously increases the wall-heat transfer. Omitting the E term (which has not a clear physical meaning) in the Jones and Launder model drastically increases the wall-heat transfer by 50%. However, the influence of E in the Chien model can be neglected. Only the Lam and Bremhorst model takes the f_1 function (which also has not a very clear physical meaning) not equal to 1; its influence is seen to be very large. The influence of the f_μ function is large for all models.

The poor performance of the To and Humphrey

(a)

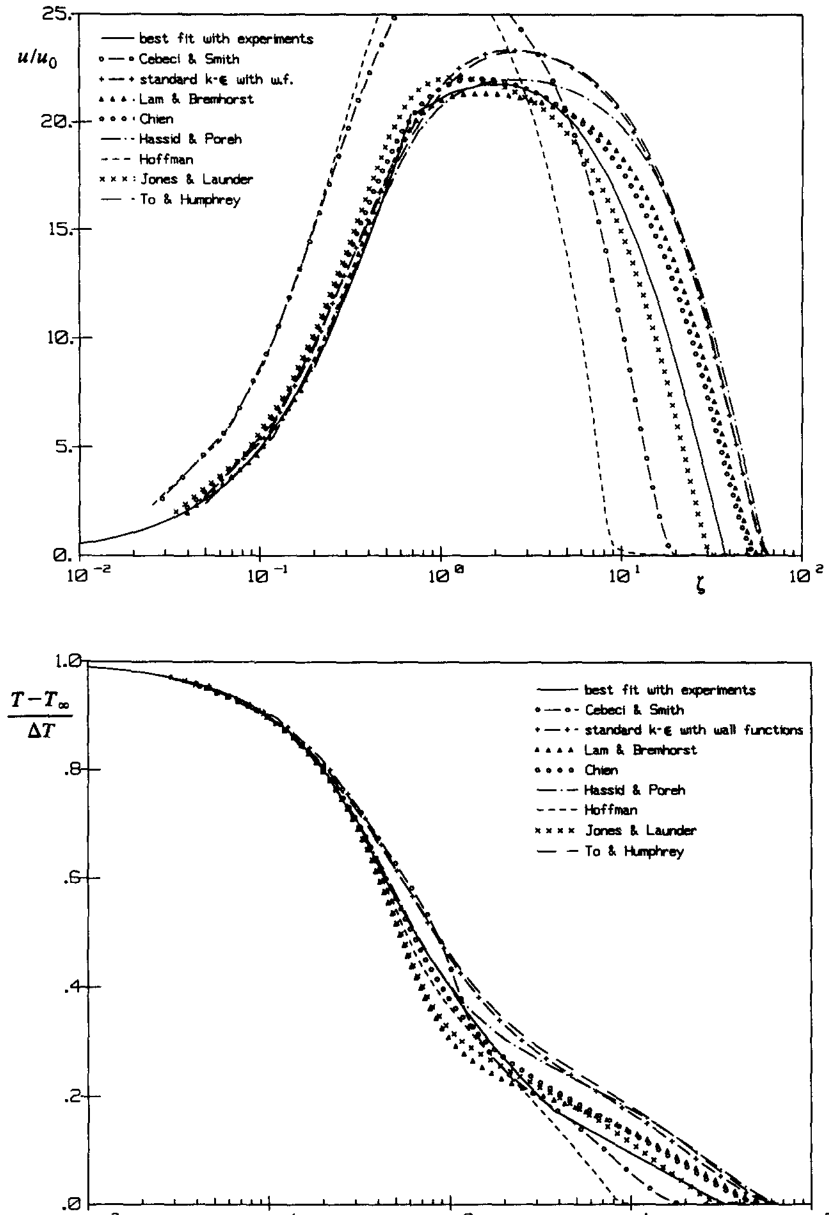

(b)

FIG. 2. Calculated velocity (a) and temperature (b) profiles.

model (Table 2), which actually is a modified Jones and Launder model, has been investigated. Firstly, To and Humphrey exchanged the D term with a non-zero boundary condition for ε at the wall, which only leads to small differences. Secondly they added a correction f_3 to the f_2 function, which was also shown to have a negligible effect. Lastly To and Humphrey omitted the E term in the Jones and Launder model; our calculations show that retaining the E term in the To and Humphrey model decreases the wall-heat transfer at $Gr_x = 10^{11}$ by 26%, giving a value close to the experimental one.

This sensitivity analysis suggests that among the low-Reynolds number k–ε models the Chien model has to be preferred, because both the Lam and Bremhorst model and the Jones and Launder model contain a term (the f_1 term and the E term, respectively) which has not a very good physical foundation, as explained in Section 2, but largely contributes to the result. A disadvantage of the Chien model is that it contains only low-Reynolds number contributions due to wall influence (except for the f_2 term, which was checked to be of negligible importance), not accounting for the low turbulence effects at the outer edge of the boundary layer. The wall-heat transfer with the standard k–ε model is largely influenced by the choice of the wall functions for k and ε. If these wall functions are replaced by zero wall conditions for k and ε, and the functions D and f_μ of Chien are added to the standard k–ε model, a new low-Reynolds

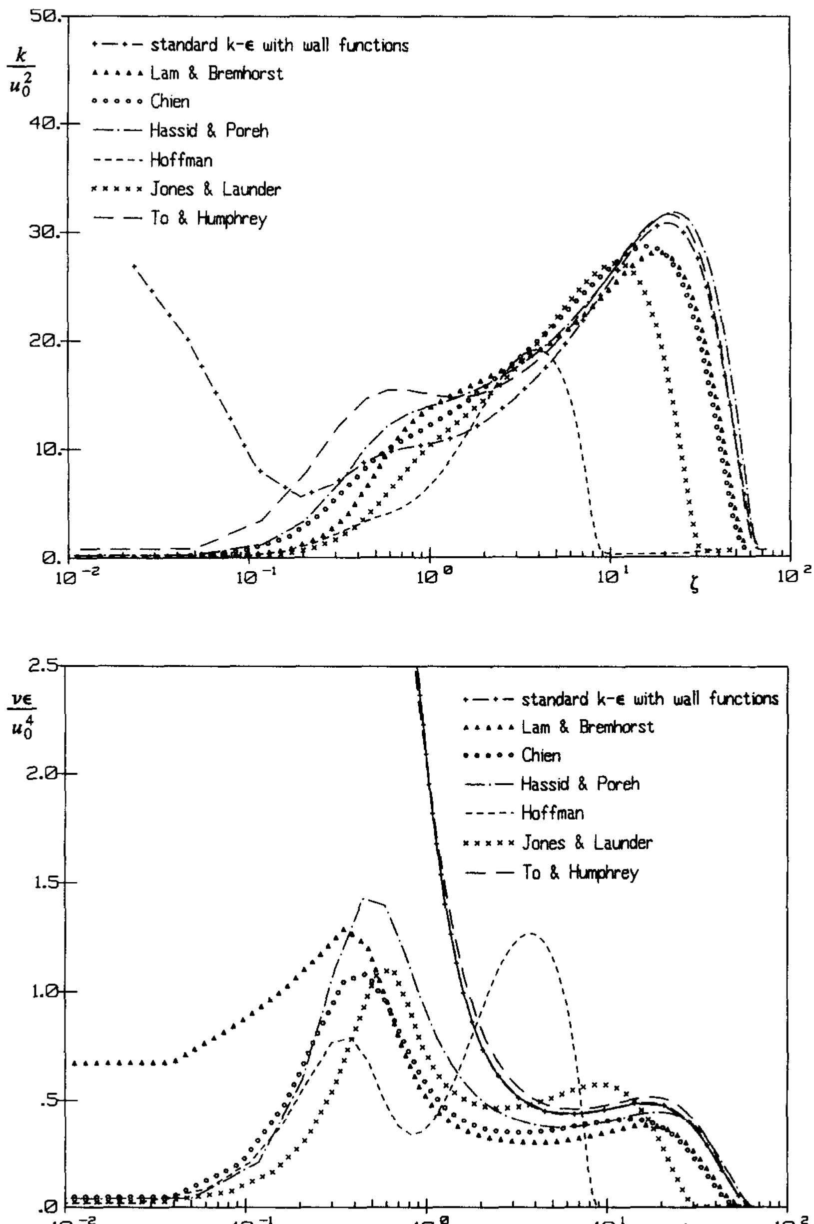

(a)

(b)

Fig. 3. Calculated turbulent quantities at $Gr_x = 10^{11}$ ($Pr = 0.72$): (a) turbulent kinetic energy; (b) rate of turbulent energy dissipation; (c) turbulent viscosity.

number k–ε model is obtained. This model calculates the turbulent natural convection boundary layer as good as the best existing low-Reynolds number k–ε models (see last variation of the Chien model in Table 3), but uses less low-Reynolds number functions.

6. CONCLUSION

If homogeneous boundary conditions for k and ε at the outer edge are applied, the solution of all low-Reynolds number k–ε models is nonunique; both a laminar and a turbulent solution can occur. The solutions of the Cebeci–Smith model and the standard k–ε model with wall functions seem to be unique.

The wall-heat transfer at $Gr_x = 10^{11}$ for air as calculated with the Cebeci–Smith model is 21% below the experimental value. The turbulent viscosity calculated with this model is much too low, resulting in a laminar-like velocity profile, having a small boundary-layer thickness and a velocity peak which is 22% above the experimental value.

The standard k–ε model with wall functions calculates a wall-heat transfer at $Gr_x = 10^{11}$ which is 30% above the experimental value. The velocity and temperature profiles with this model are only slightly worse than with the best low-Reynolds number k–ε models. The velocity maximum is too high and its position is too far from the wall.

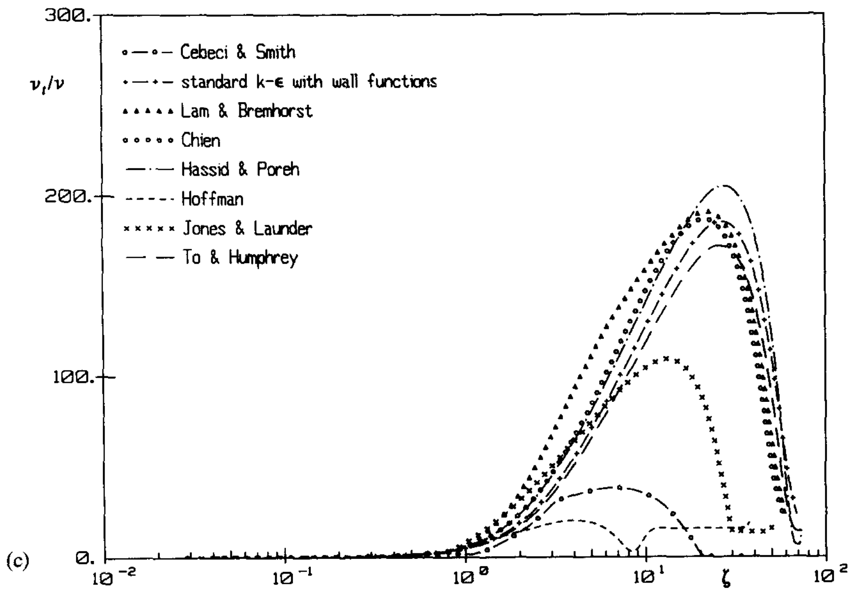

FIG. 3.—*Continued.*

The models of Lam and Bremhorst, Chien, and Jones and Launder are the low-Reynolds number k–ε models giving the best results in describing the velocity profiles for the natural convection boundary layer flow of air. Patel *et al.* concluded the same for the forced convection boundary layer. At $Gr_x = 10^{11}$ the wall-heat transfer deviates by only a few percent from the experimental value. For larger Grashof numbers the Jones and Launder model gives the best wall-heat transfer predictions.

Accurate heat-transfer calculations for a natural convection boundary layer require the introduction of low-Reynolds number terms in the standard k–ε model. The algebraic model of Cebeci–Smith and the use of existing wall functions for k and ε in the standard k–ε model lead to a limited accuracy. Replacing these wall functions by zero wall conditions for k and ε and extending the standard k–ε model with Chien's D and f_μ terms gives a simple low-Reynolds number k–ε model. It uses less functions

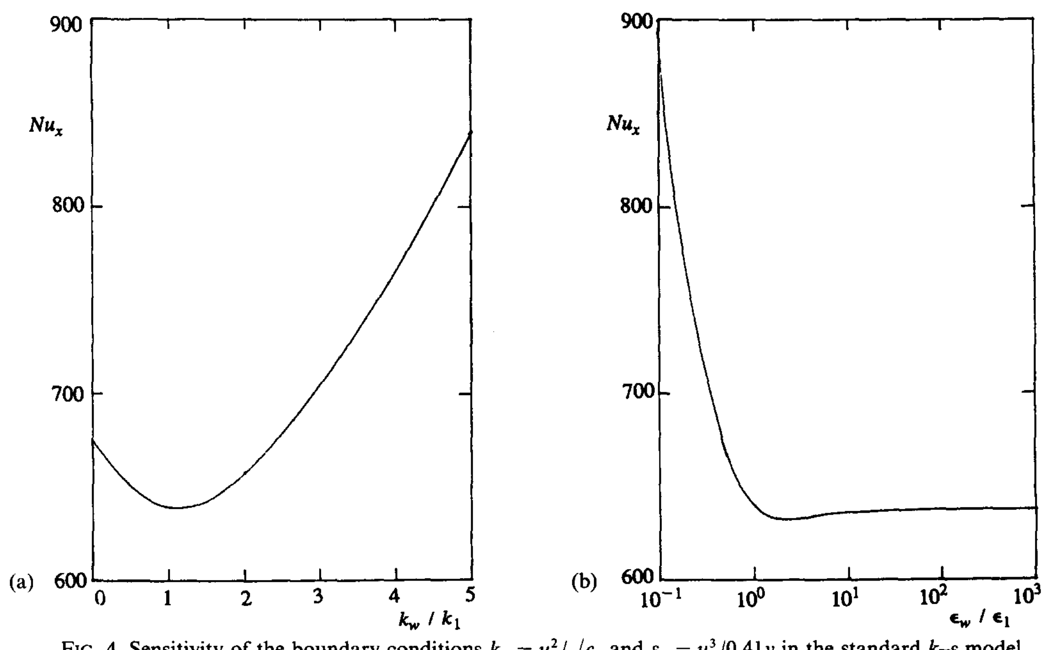

FIG. 4. Sensitivity of the boundary conditions $k_1 = u_\tau^2/\sqrt{c_\mu}$ and $\varepsilon_1 = u_\tau^3/0.41y$ in the standard k–ε model ($Gr_x = 10^{11}$, $Pr = 0.72$): (a) ε_w fixed at $\varepsilon_1 = u_\tau^3/0.41y$; (b) k_w fixed at $k_1 = u_\tau^2/\sqrt{c_\mu}$.

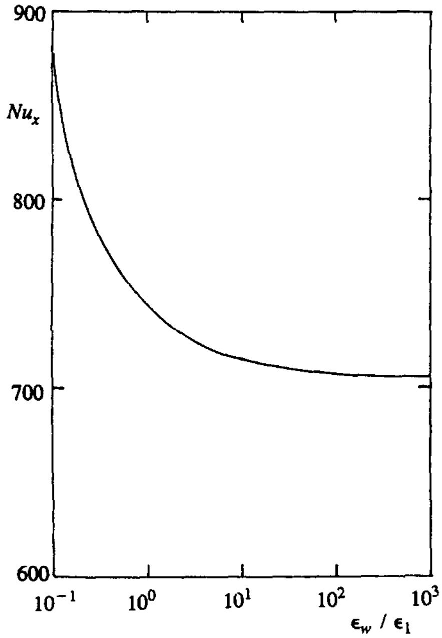

FIG. 5. Sensitivity of the boundary condition $\varepsilon_1 = c_\mu^{3/4}k^{3/2}/0.41y$ in the standard k–ε model ($k_w = 0$, $Gr_x = 10^{11}$, $Pr = 0.72$).

Table 3. Influence on the wall-heat transfer of the different terms in the low-Reynolds number k–ε models ($Gr_x = 10^{11}$, $Pr = 0.72$)

Variation	Nu_x
(a) Lam and Bremhorst model	
None	541
$f_\mu = 1$, but f_3 unchanged	9%
$f_1 = 1$	45%
$f_2 = 1$	0%
$\varepsilon_w = 0$, $D = -2\nu(\partial\sqrt{k}/\partial y)^2$	2%
$\varepsilon_w = 0$, $D = -2\nu k/y^2$	−9%
$\varepsilon_w = 0$	0%
(b) Chien model	
None	543
$f_\mu = 1$	13%
$f_2 = 1$	0%
$E = 0$	0%
$D = D_{\text{Chien}}/4$	24%
$\varepsilon_w = \nu(\partial^2 k/\partial y^2)_w$, $D = 0$	9%
$c_{1\varepsilon} = 1.44$, $c_{2\varepsilon} = 1.92$	−3%
$c_{1\varepsilon} = 1.44$, $c_{2\varepsilon} = 1.92$, $E = 0$, $f_1 = f_2 = 1$	−3%
(c) Jones and Launder model	
None	465
$f_\mu = 1$	23%
$f_2 = 1$	0%
$E = 0$	50%
$D = 0$	6%
$\varepsilon_w = 2\nu(\partial\sqrt{k}/\partial y)_w^2$, $D = 0$	3%

than existing models, but has the same accuracy as the models of Lam and Bremhorst, Chien, and Jones and Launder.

REFERENCES

1. B. E. Launder, Numerical computation of convective heat transfer in complex turbulent flows: time to abandon wall functions?, *Int. J. Heat Mass Transfer* **27**, 1485–1491 (1984).
2. L. Prandtl, Uber Flüssigkeitsbewegung bei sehr kleiner Reibung, *Proc. 3rd Int. Math. Congr.*, Heidelberg (1904). Reprinted in: *Vier Abhandlungen zur Hydro- und Aerodynamik*, Göttingen (1927); NACA TM 452 (1928); see also *Coll. Works*, Vol. II, pp. 575–584 (1961).
3. V. C. Patel, W. Rodi and G. Scheuerer, Evaluation of turbulence models for near-wall and low-Reynolds number flows, *Proc. 3rd Symp. Turbulent Shear Flows*, California (1981).
4. V. C. Patel, W. Rodi and G. Scheuerer, Turbulence models for near-wall and low-Reynolds number flows: a review, *AIAA J.* **23,** 1308–1319 (1985).
5. W. K. George and S. P. Capp, A theory for natural convection turbulent boundary layers next to heated vertical surfaces, *Int. J. Heat Mass Transfer* **22,** 813–826 (1979).
6. R. Cheesewright, The scaling of turbulent natural convection boundary layers in the asymptotic limit of infinite Grashof number, paper presented at Euromech Colloquium 207, 7–9 April, Delft, The Netherlands (1986).
7. C. K. G. Lam and K. Bremhorst, A modified form of the k–ε model for predicting wall turbulence, *J. Fluids Engng* **103,** 456–460 (1981).
8. K.-Y. Chien, Predictions of channel and boundary layer flows with a low-Reynolds-number two-equation model of turbulence, AIAA-80-0134 (1980).
9. K.-Y. Chien, Predictions of channel and boundary-layer flows with a low-Reynolds-number turbulence model, *AIAA J.* **20,** 33–38 (1982).
10. W. P. Jones and B. E. Launder, The prediction of laminarization with a two-equation model of turbulence, *Int. J. Heat Mass Transfer* **15,** 301–314 (1972).
11. T. Cebeci and A. M. O. Smith, *Analysis of Turbulent Boundary Layers*. Academic Press, New York (1974).
12. T. Cebeci and A. Khattab, Prediction of turbulent-free-convective-heat transfer from a vertical flat plate, *J. Heat Transfer* **97,** 469–471 (1975).
13. S.-J. Lin and S. W. Churchill, Turbulent free convection from a vertical, isothermal plate, *Numer. Heat Transfer* **1,** 129–145 (1978).
14. S. Hassid and M. Poreh, A turbulent energy dissipation model for flows with drag reduction, *J. Fluids Engng* **100,** 107–112 (1978).
15. W. C. Reynolds, Computation of turbulent flows, *Ann. Rev. Fluid Mech.* **8,** 183–208 (1976).
16. G. H. Hoffman, Improved form of the low Reynolds number k–ε turbulence model, *Physics Fluids* **18,** 309–312 (1975).
17. W. M. To and J. A. C. Humphrey, Numerical simulation of buoyant, turbulent flow—1. Free convection along a heated, vertical, flat plate, *Int. J. Heat Mass Transfer* **29,** 573–592 (1986).
18. S. P. Vanka, Block-implicit calculation of steady turbulent recirculating flows, *Int. J. Heat Mass Transfer* **28,** 2093–2103 (1985).
19. H. Ozoe, A. Mouri, M. Ohmuro, S. W. Churchill and N. Lior, Numerical calculations of laminar and turbulent natural convection in water in rectangular channels heated and cooled isothermally on the opposing vertical walls, *Int. J. Heat Mass Transfer* **28,** 125–138 (1985).
20. R. Cheesewright, Turbulent natural convection from a vertical plane surface, *J. Heat Transfer* **90,** 1–8 (1968).

21. R. Cheesewright and E. Ierokipiotis, Velocity measurements in a natural convection boundary layer, Queen Mary College, Faculty of Engineering Research, Report EP 5022 (1981).
22. R. Cheesewright and E. Ierokipiotis, Velocity measurements in a turbulent natural convection boundary layer, *Proc. 7th Int. Heat Transfer Conf.*, Vol. 2, pp. 305–309. Munich, F.R.G. (1982).
23. M. Miyamoto, H. Kajino, J. Kurima and I. Takanami, Development of turbulence characteristics in a vertical free convection boundary layer, *Proc. 7th Int. Heat Transfer Conf.*, pp. 323–328 (1982).
24. M. Miyamoto, Y. Katoh, J. Kurima and H. Kajino, An experimental study of turbulent free convection boundary layer along a vertical surface using LDV, *Proc. Osaka Symp.*, 15 July, Osaka, Japan (1983).
25. D. L. Siebers, R. F. Moffatt and R. G. Schwind, Experimental, variable properties natural convection from a large, vertical flat surface, *J. Heat Transfer* **107**, 124–132 (1985).
26. J. P. Coulter and S. I. Guceri, Laminar and turbulent natural convection in irregularly shaped enclosures, CAE Report-3/85, Department of Mechanical and Aerospace Engineering, University of Delaware (1985).

COMPARAISON DES MODELES DE TURBULENCE POUR LA COUCHE LIMITE DE CONVECTION NATURELLE LE LONG D'UNE PLAQUE CHAUDE VERTICALE

Résumé—Avec un code numérique pour résoudre les équations de couche limite, les performances de différents modèles de turbulence sont testés pour la couche limite de convection naturelle d'air le long d'une plaque chaude et verticale. On a testé le modèle algébrique Cebeci–Smith, le modèle standard k–ε avec des fonctions de paroi pour k et ε et différents modèles k–ε à faible nombre de Reynolds. Le modèle Cebeci–Smith calcule un transfert thermique pariétal et une viscosité turbulente trop faibles. Le modèle k–ε standard avec des fonctions de paroi donne un transfert à la paroi trop élevé, mais les profils de vitesse et de température sont en accord raisonnable avec les expériences. Des résultats précis de transfert à la paroi requièrent l'utilisation des modèles k–ε à faible nombre de Reynolds; les modèles de Lam et Bremhorst, de Chien, de Jones et Launder conviennent jusqu'à un nombre de Grashof de 10^{11}. Pour des nombres de Grashof plus grands, le modèle de Jones et Launder est meilleur. Une étude de sensibilité montre que le transfert thermique à la paroi avec le modèle standard k–ε dépend largement du choix des fonctions de paroi pour k et ε. Le remplacement de ces fonctions par des conditions de zéro à la paroi pour k et ε et l'addition des fonctions D et f_μ du modèle de Chien au modèle k–ε standard, donnent un modèle simple et précis pour la couche limite de convection naturelle.

VERGLEICH VON TURBULENZMODELLEN FÜR DIE GRENZSCHICHT DER NATÜRLICHEN KONVEKTION AN EINER BEHEIZTEN VERTIKALEN PLATTE

Zusammenfassung—Mit Hilfe eines numerischen Rechenprogramms zur Lösung von Grenzschichtproblemen wurde die Anwendung von verschiedenen Turbulenzmodellen für die Grenzschicht der natürlichen Konvektion von Luft an einer beheizten vertikalen Platte überprüft. Untersucht wurde das Cebeci–Smith-Modell, das Standard k–ε-Modell mit Wandfunktionen für k und ε und unterschiedliche k–ε-Modelle für geringe Reynolds-Zahlen. Das Cebeci–Smith Modell errechnet einen zu geringen Wärmeübergang an der Wand und eine zu geringe turbulente Viskosität. Das Standard k–ε-Modell ergibt einen zu hohen Wärmeübergang an der Wand—die Geschwindigkeits- und Temperaturprofile stimmen jedoch gut mit den Experimenten überein. Um den Wärmeübergang an der Wand richtig zu berechnen, muß ein k–ε-Modell für geringe Reynolds-Zahlen benutzt werden. Dabei liefern die Modelle von Lam und Bremhorst, Chien, Jones und Launder die besten Ergebnisse bis zu Grashof-Zahlen von 10^{11}. Für größere Grashof-Zahlen ist das Modell von Jones und Launder das beste. Eine Parameterstudie zeigt, daß der Wärmeübergang an der Wand beim Standard-k–ε-Modell sehr stark von der Wahl der Wandfunktion k und ε abhängt. Setzt man diese Wandfunktionen zu 0 und erweitert das Standard-k–ε-Modell um die Funktionen D und f_μ aus dem Chien-Modell, so erhält man ein genaues k–ε-Modell für kleine Reynolds-Zahlen für die Grenzschicht der natürlichen Konvektion.

СРАВНЕНИЕ МОДЕЛЕЙ ТУРБУЛЕНТНОСТИ, ИСПОЛЬЗУЕМЫХ ДЛЯ РАСЧЕТА ПОГРАНИЧНОГО СЛОЯ У НАГРЕТОЙ ВЕРТИКАЛЬНОЙ ПЛАСТИНЫ ПРИ ЕСТЕСТВЕННОЙ КОНВЕКЦИИ

Аннотация—При помощи численной схемы, используемой для решения уравнений пограничного слоя, исследуется адекватность различных моделей турбулентности для расчета пограничного слоя воздуха у нагретой вертикальной пластины в условиях естественной конвекции. Анализируются алгебраическая модель Цебеси–Смита, обычная модель k–ε с пристенными функциями для k и ε и различные модели k–ε для низких чисел Рейнольдса. Модель Цебеси–Смита дает весьма заниженные значения теплового потока на стенке и турбулентной вязкости. Обычная модель k–ε с пристенными функциями дает очень высокие значения теплового потока на стенке, однако профили скорости и температуры достаточно хорошо согласуются с экспериментальными данными. Наиболее точное определение теплового потока на стенке требует использования низкорейнольдсовых моделей k–ε; модели Лэма и Бремхорста, Чена, а также Джонса и Лаундера дают наилучшие результаты для чисел Грасгофа, не превышающих 10^{11}. Выше этого значения лучше всего подходит модель Джонса и Лаундера. Показано, что теплоперенос на стенке, рассчитанный по стандартной модели k–ε, сильно зависит от выбора пристенных функций для k и ε. Замена этих функций нулевыми условиями для k и ε и ввод функций модели Чена D и f_μ в обычную модель k–ε дает простую, но достаточно строгую модель k–ε для низких чисел Рейнольдса в случае естественной конвекции в пограничном слое.